Statistical Study for Optimization Magnetic Property of Modified MNPs (Fe_3O_4/PEG(PVA)) Synthesis by Co-Precipitation Method

Khodadadi, Abolfazl*+

Department of Physics, Tehran North Branch, Islamic Azad University, Tehran, I.R. IRAN

Talebtash, Mohammad Rahim

Department of Engineering, Shahriar Branch, Islamic Azad University, Shahriar, I.R. IRAN

Farahmandjou, Majid

Departments of Physics, Varamin-Pishva Branch, Islamic Azad University, Varamin, I.R. IRAN

Behnam Saba, Ahmad Reza

Department of Chemistry, Payame Noor University, Tehran, I.R. IRAN

ABSTRACT: *In this research, MNPs were fabricated and coated by the co-precipitation method. The study of this process was performed in a two-level factorial design framework. The effect of a polymeric agent, the strength of the alkaline solution, and the temperature on the magnetic properties MNPs were studied in this design. the structure, morphology, size, appearance, and magnetic behavior of modified MNPs were investigated using XRD, FT-IR, TEM, and VSM. The results obtained from the spectra show the modified MNPs have superparamagnetic behavior with high saturation magnetization (M_s) and small coercivity (H_c). The mean size of coated MNPs was determined 10 nm, saturation magnetization 60.98 emu/g, and magnetic coercivity 8.26 G.*

KEYWORD: *Two-level factorial design; Saturation magnetization; Magnetic coercivity; Remanent magnetization.*

INTRODUCTION

Magnetic NanoParticles (MNPs) are one of the most important groups in the field of nanoparticles. MNPs have significant physical and chemical properties related to their morphology, size, and magnetic saturation. Researchers are increasingly considering these MNPs depending on these properties [1-5]. Magnetic nanoparticles are easily separated under the influence of an external magnetic field, a property that can be used in various medical and industrial fields [6-11].

Iron oxide (Fe_3O_4) is found in 16 different structures. The most important forms are magnetite and maghemite due to their specific magnetic properties. Magnetite

has better magnetic saturation. The color of magnetite is black and the most important elements in the structure of magnetite are both iron oxidation states II and III [12,13].

MNPs have many applications in the petroleum industry, including in the field of targeted absorption, remote detection and transmission, and local heating. Also, MNPs can be used as adsorbents for solid-phase extraction. In magnetic solid phase extraction, MNPs are added to the solution containing the sample to be analyzed, and during the process, the desired material is absorbed by the MNPs and separated by a separator (magnet). Another important use is in the high-density media for magnetic storage devices with a perpendicular type of magnetization [14,15].

MNPs can be fabricated by both physical and chemical methods. Although physical methods (from top to bottom) are scalable, cost-effective and capable of industrial production, in some methods, such as the steam condensation method, they have disadvantages such as exothermicity and oxidation. Also, a significant amount of mechanical, thermal or electrical energy is needed to transform materials into nanoparticles [16]. The chemical methods (from bottom to top) have a higher capability due to better control of synthesis parameters (temperature, molar ratio of raw materials, pH). So, the chemical method has a unique ability in the field of technology and science of nanostructured materials due to the arrangement of materials in nanometer conditions in order to achieve the desired properties, and most chemical methods follow the nucleation and growth mechanism. Sol-gel, sonochemistry, hydrothermal, microemulsion and co-precipitation are the methods of chemical synthesis [17-23].

Co-precipitation method is more suitable than other methods, due to the simplicity of the synthesis method, short reaction time, production of products with high purity, etc. In addition, it is used in most medical and industrial fields [24-27].

The ion interactions of Fe^{+2} to Fe^{+3} in the atmosphere reduces the quality of the formational magnetite [27,28]. In addition, there are strong magnetostatic, neighboring interactions and van der Waals attraction forces between MNPs. These forces sometimes cause them to aggregate and become unstable. This problem can be largely solved by reducing the size of MNPs or by using such materials as silane-based compounds, metals, polymers, and fatty and amino acids for coating and stabilizing the surface of Fe_3O_4 NPs [29-30].

In fact, The MNPs agglomeration can be avoided by creating electrostatic or spatial repulsion forces between nanoparticles in the synthesis process. Nanoparticle surface modification is done by using inorganic and organic agents [31,32].

In 2020, *Antarnusa et al.* synthesized MNPs by co-precipitation method and used $FeCl_3.6H_2O$ and $FeSO_4.7H_2O$ ammonium solution and coated them with polyethylene glycol (PEG). They used these MNPs in biosensors [33]. This process was performed under atmospheric conditions. However, the formation of other phases of magnetite diminishes the magnetic properties.

In 2019, *Ali Maleki et al.* used PVA coating agent to modify and optimize the surface of the iron oxide nanoparticles-precipitation method. They used ferrous chloride tetrahydrate, ferric chloride hexahydrate, and ammonia solution to synthesize nanoparticles. The saturation magnetization at about 40 (emu/g) and nanoparticle size at about 47nm were determined by them. It did not achieve outstanding results by this mean, because MNPs somewhat agglomerated [34].

These reports indicate that most researchers studying the optimization of the magnetic properties of coated MNPs focused on one factor at a time. The two-level factorial design method allows two or more variable factors to be examined in an experiment simultaneously. In addition, the use of this method decreases the number of experiments and reduces time consumable, cost saving, and consideration of possible interactions between factors [35-37]. *Susan Sadeghi et al.,* modified the surface of magnetic nanoparticles by using silicon. They used modified nanoparticles as adsorbents in the uranium extraction process in an aqueous medium and placed the experimental in the framework of a statistical design. using this design reduced the number of experiments to achieve their aim. They applied statistical calculations to analyze their data and obtained good results. [38]. PEG-modified magnetic nanoparticles were used by *Saba et al.*, to adsorb zirconium in a two-level factorial design. They used modified MNPs to adsorb and separate Zr(IV) ions in aqueous solution, but the optimization of these kinds of coated nanoparticles as a substrate was not observed in their studies [39].

In order to investigate the magnetic behavior of the modified MNPs in a new design by co-precipitation method (in situ), the synthesis process of the modified

Research Article

Table1: Factors, their symbols and levels for central composite design.

Factors	Symbol	level		
		-1	0	+1
Kinds of alkaline agents	A	NaOH solution	50% NaOH ,50% NH$_3$	NH$_3$ solution
Kinds of coating agents	B	PEG polymeric	90% PEG ,10%PVA	PVA polymeric
Kinds of temperatures	C	20℃	50℃	80℃

nanoparticles were performed. Optimization of MNPs was carried out within the framework of a two-level factorial design. The coating agents (PEG and PVA), strong alkaline solution (NH$_4$OH and NaOH), and temperature (low and high) are considered for this novel design. According to studies, such a design has not been used to optimize magnetic properties. Therefore, the modification and optimization of magnetic nanoparticles based on a two-level factorial design is completely new and innovative.

STATISTICAL DESIGN

A full two-level factorial design was performed to investigate the effect of effective factors or interaction between two or more factors on the response. Using this method, the magnetic behavior of nanoparticles in some cases can be estimated, this can be provided by an empirical mathematical model.

The saturation magnetization(or remanent magnetization) of coated MNPs efficiently is a response variable.

three main factors consist of the polymer agent, alkaline solution, and temperature. They were applied in a two-level factorial design. Thus 2^3=8 sets of experimental were required to analyze the factors and their interaction effects.

In this design the minimum, central point, and maximum for each factor were coded with -1, 0, +1; respectively. Twice experiments under defined conditions did in order to take values of the central point. The results of these duplicated experiments were used to estimate the standard deviation of effects. These results determined the effectiveness of the factor through the selected range [40]. The levels and factors mentioned are listed in Table 1.

EXPERIMENTAL SECTION
Materials and equipment

Ferric chloride hexahydrate (FeCl$_3$.6H$_2$O) (%99), ferrous chloride tetrahydrate ($FeCl_2 \cdot 4H_2O$) (%99),

chloric acid (HCl) (%37), ammonia solution (NH_4OH) (%25), distilled water, polyethylene glycol (PEG-1000) and polyvinyl alcohol (PVA) have been used to synthesize pure and modified MNPs.

Equipment includes a digital scale with an accuracy of 0.0001 g (model KF3004), Hidolph magnetic stirrer HEI-TEC0145, Electrothermal EM1000CE, HANNA digital potentiometer Hi 2211, an oven BM120E and a digital thermometer STC-100A.

The structural study was performed by X-ray diffraction (XRD) and data with 2θ in the angle range 10 to 70 degrees (with the type X-Pert Pro MPD, Cu-Kα (λ = 1.54060 A °) was recorded. The transmission of the optical spectrum in the infrared spectrum (FT-IR) was performed by a Spectrum RXI Infrared Fourier Transform Spectrometer manufactured by Perkin Elmer. The appearance and average size of nanoparticles were determined by transmission electron microscopy (TEM) with Zeiss EM-900 model (80 kV). The magnetic behavior of the samples was evaluated by a vibrating sample magnetometer (VSM) with the Lake Shore 7400 model at room temperature.

Synthesis of magnetic nanoparticles

Pure and modified MNPs have been synthesized by the co-precipitation method with F$eCl_3.6H_2O$ and $FeCl_2.4H_2O$ precursors. PEG and PVA polymeric agents were used to modify the surface of MNPs.

To produce a pure sample, first, $FeCl_3.6H_2O$ (2.71 gr) and $FeCl_2 \cdot 4H_2O$ (1.1gr) have been mixed in a 2:1 ratio in a three-necked flask. Then, 15.1 HCl (0.5 M) was added and stirred at 350 rpm. At 80 °C, this mixed solution was deoxygenized by nitrogen gas for 25 min. A nitrogen gas capsule was used to inject N_2 gas into the reactor at an injection rate of 3 L/min. Simultaneously, in the second flask, the ammonium solution (2M) was deoxygenated with nitrogen gas for 25 min. the mixed solution added
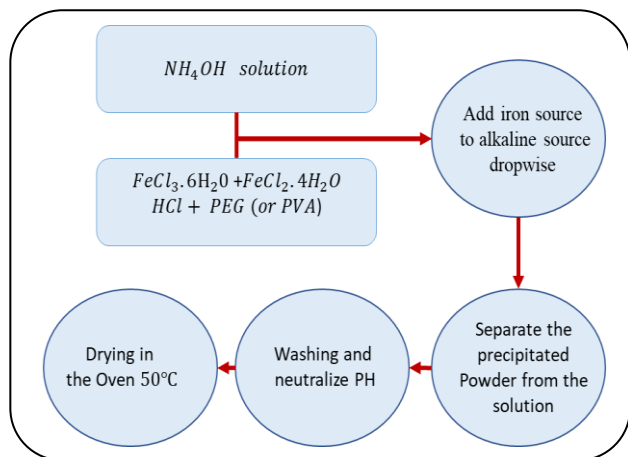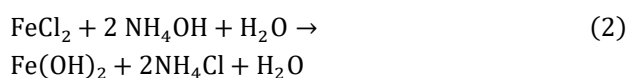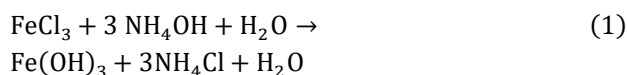
Fig. 1: Flowchart of coating MNPs

dropwise to the alkaline solution. Gradually, by adding any drop, a suspension MNPs were formed at a pH=13. MNPs were separated from the solution, by an external magnetic field. The product was washed several times by water to reach pH=7. Then it was dried at 50 ° C by an oven.

Eq.1 to Eq.3 express the chemical equation to produce pure MNPs.

$$FeCl_3 + 3\ NH_4OH + H_2O \rightarrow \qquad (1)$$
$$Fe(OH)_3 + 3NH_4Cl + H_2O$$

$$FeCl_2 + 2\ NH_4OH + H_2O \rightarrow \qquad (2)$$
$$Fe(OH)_2 + 2NH_4Cl + H_2O$$

$$Fe(OH)_2 + 2Fe(OH)_3 \rightarrow \qquad (3)$$
$$Fe_3O_4 + 4H_2O$$

To produce coated MNPs, first, $FeCl_3.6H_2O$, $FeCl_2 \cdot 4H_2O$ in a 2:1 ratio and 3g PEG (or 0.5 gr PVA) have been mixed in a three-necked flask. Then it was dissolved in 15cc HCl (0.5 M) under a magnetic stirrer at 350 rpm.

Similar to the pure sample production process, ammonium solution (2M) was prepared and it was added dropwise to the flask. Other synthesis steps were performed similarly to the previous process (Fig.1). The resulting powders were prepared for different spectra, such as XRD, SEM, TEM, FT-IR and VSM.

RESULTS AND DISCUSSION
Investigation of magnetic properties of coated magnetic nanoparticles

Fig. 2, represents the XRD analysis of the coated MNPs. The crystal structure, phases and particle size of MNPs were studied at room temperature. As can be seen

in the XRD images, similar to the structure of pure MNPs, the crystal structure of PEG-coated MNPs was face center cubic (FCC) and the molecular structure of the reverse spinel. The lattice constant was 8.34 Å, and unit cell comprising 24 Fe atoms and 32 O atoms. The peaks in the XRD spectra were located at angles 2θ =30/1°(220), 35/3°(311),43/2°(400) ,53/2°(422),57/3°(511), 62/6°(440). These data perfectly compatible with the magnetite-related values of JCPS (19629) card.

The peaks in the XRD spectra of PVA-coated MNPs shows magnetic and amorphous contribution. The crystal structure of coated sample was cubic spinel and the lattice parameters were a = b = c = 8.360 Å. The Fe^{+3} and Fe^{+2} cations occupied all tetrahedral and half of the octahedral sites in crystal, respectively.

The main sharp peaks were at angles $2\theta = 31.17°(220)$, $35.5°(311)$, $43,5°(400)$, $52.5°(422)$, $57.4°(511)$, $63.16°(440)$. In addition, at $2\theta = 19.2°$, the amorphous phase diffraction peak was appeared and indicates the presence of PVA in sample. These data perfectly compatible with the magnetite-related values of JCPS (65-3107) card. According to the Scherrer's equation (Eq.4), the size of the coated MNPs by PVA and PEG agents were calculated about 19 nm and 11 nm, respectively [41].

$$d = \frac{0.9\lambda}{\beta COS\theta} \qquad (4)$$

It is clear that the polymer agent places on the surface of MNPs and prevents to growth of them, thereby reducing the size of the nanoparticles.

The Fourier Transform InfraRed (FT-IR) spectroscopy analysis was applied to determine the functional group and vibrational bonds in samples. Fig.3 shows the FT-IR analysis of PEG, pure and PEG-coated MNPs.

Three peaks at 570.98 cm^{-1} , $1627.0 cm^{-1}$ and $3431.21 cm^{-1}$ appeared in the spectrum of pure MNPs. The peak at $1627.0 cm^{-1}$ were attributed to the bending vibration of the water absorption from the surface of Fe_3O_4 MNPs. In FT-IR spectra of PEG, the absorption peak at $3451.17 cm^{-1}$, $1467 cm^{-1}$ and $1111.3 cm^{-1}$ are related to the tensile bands OH, the bending band C-OH and the tensile band C-O-C, respectively. The other peaks are in the fingerprint region [42,43].

The absorption bands in the regions of $874.21 cm^{-1}$ until $1384.4 cm^{-1}$ were present in PEG polymer agent

spectrum, while were absent in pure sample spectrum. Accordingly, the present of these bonds in PEG-coated sample, indicates the PEG linked on the surface of MNPs.

Similarly, Fig.4, shows the FT-IR analysis of PVA-coated MNPs. In FT-IR spectra of PVA, the peak at $3364/25 Cm^{-1}$ was related to the vibrating banner O-H. the strong peak absorption band at $2879/40 Cm^{-1}$ indicates an asymmetric tensile vibration in the C-H groups. The strong peak at $1111/81 Cm^{-1}$ was related to the vibration band Fe-O-C, corresponding to the interaction between the polymer agent and magnetite nanoparticles. So, this peak indicated the placement of PVA polymer agent on the surface of MNPs.

TEM analysis was conducted to determine the precise size and appearance of MNPs. Fig.5 shows the TEM analysis of MNPs coated with both PVA and PEG polymeric agents. As can be seen, the shape of the MNPs were almost spherical and they are somewhat stuck, as a result of the electrostatic repulsion and steric hindrance force [44,45]. The mean size of coated MNPs with PEG and PVA were determined 10 nm and 20 nm respectively.

The size of coated MNPs is less than 20 nm, according to the documentation, coated MNPs have super paramagnetic properties [44,46].

To investigate the magnetic behavior of coated MNPs, the VSM analysis was performed. The role of each factor such as coating agent, the strength of alkali solution and temperature on the magnetic properties of coated MNPs were studied. The amount of saturation magnetization, magnetic remanent and coercive force of each sample in different conditions were analyzed and compared. The results indicate that the coated MNPs have the behavior of super paramagnetic materials (Fig. 6).

The Fig. 7 shows that the increasing temperature (below the Curie temperature) directly increase the saturation magnetization of coated MNPs. The amount of saturated magnetization is significantly higher when PEG coating agent is used. Due to the use of diamagnetic coating and reduced particle size of the nanoparticles, the amount of magnetic saturation of the modified nanoparticles is less than of pure magnetic nanoparticles [47-49]. The effect of polymer agent and temperature on the magnetic remanent of magnetic nanoparticles is evaluated according to the diagrams Fig.8.
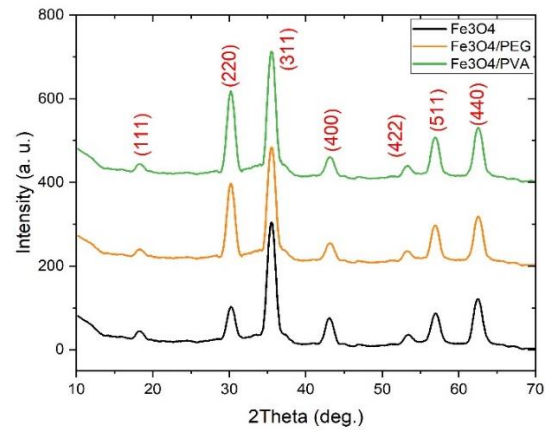

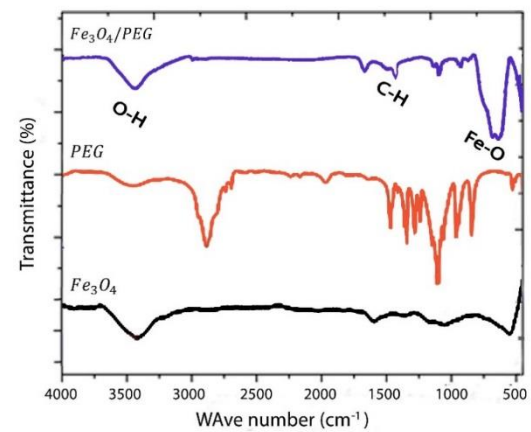*Fig. 2: XRD spectrum of pure and coated magnetic nanoparticles.*

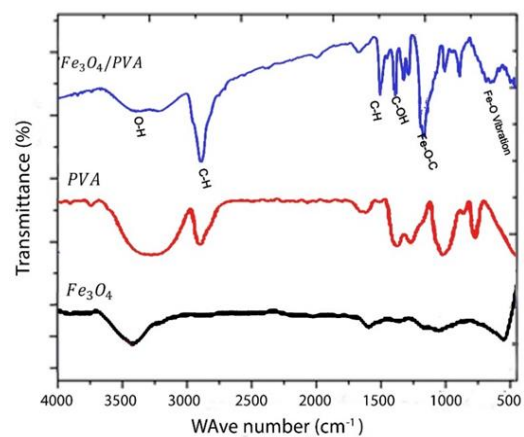*Fig. 3. The FT-IR analysis of PEG, pure and PEG-coated MNPs.*

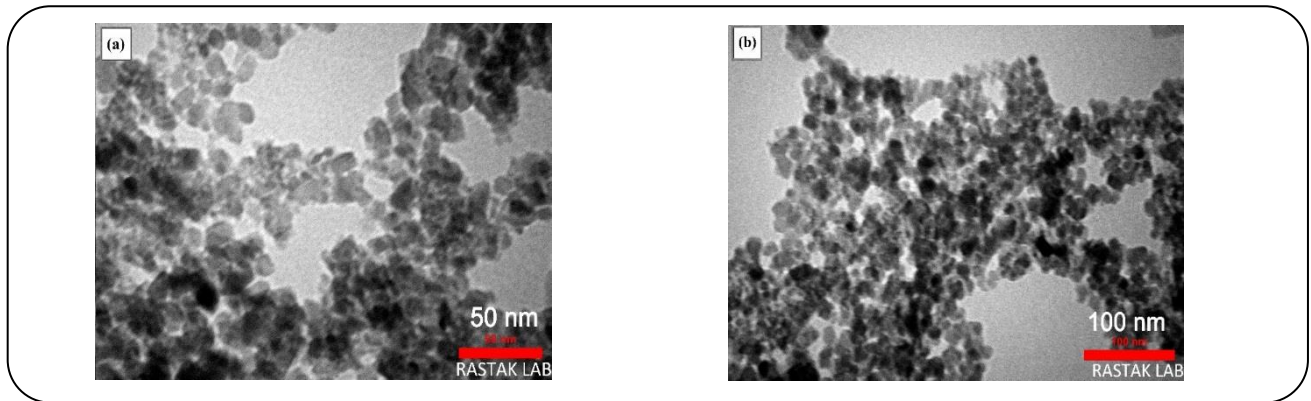*Fig. 4: The FT-IR analysis of PVA, pure and PVA-coated MNPs.*

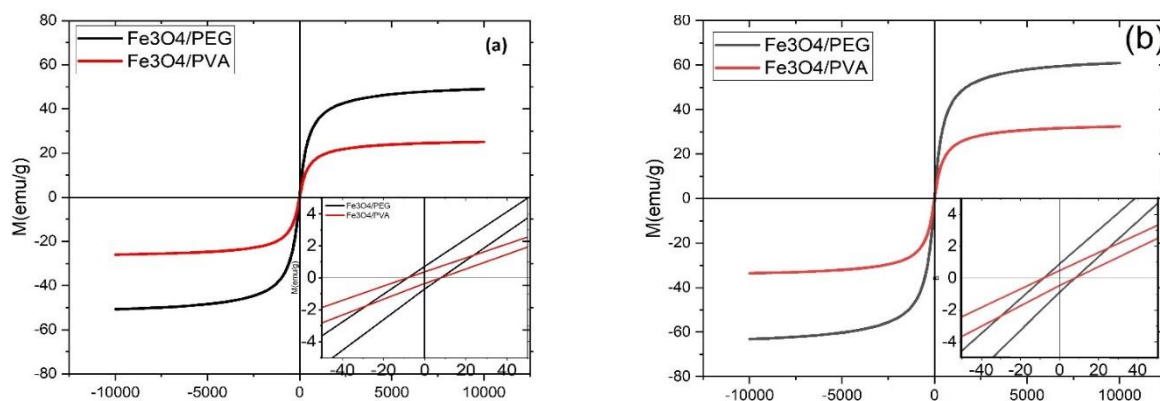*Fig. 5: TEM analysis (a) Fe_3O_4 / PEG (b) Fe_3O_4 / PVA.*

Fig. 6: VSM analysis related to Fe_3O_4 / PEG and Fe_3O_4 / PVA nanoparticles at (a) 20 • and (b) 80 • C.
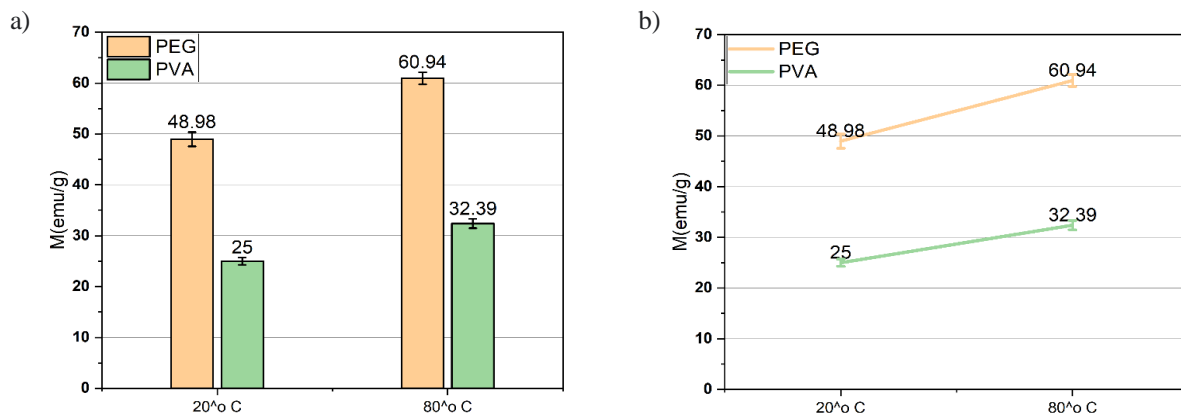

Fig. 7: Investigation of the effect of coating factor and temperature on saturation magnetism.

Modified nanoparticles with PEG polymer agent provide higher stability, because by stopping the growth process, they preserve the synthesized magnetite nanoparticles at the nanoscale. The presence of electrostatic attraction and hydrogen bonds causes the polymeric agent to stick to the surface of the nanoparticles and not easily separate from the surface. The intensity of the effect of this result was lower for Modified nanoparticles with PVA polymer agent.

Table 2: Calculated M_s from results of coded designed experiments.

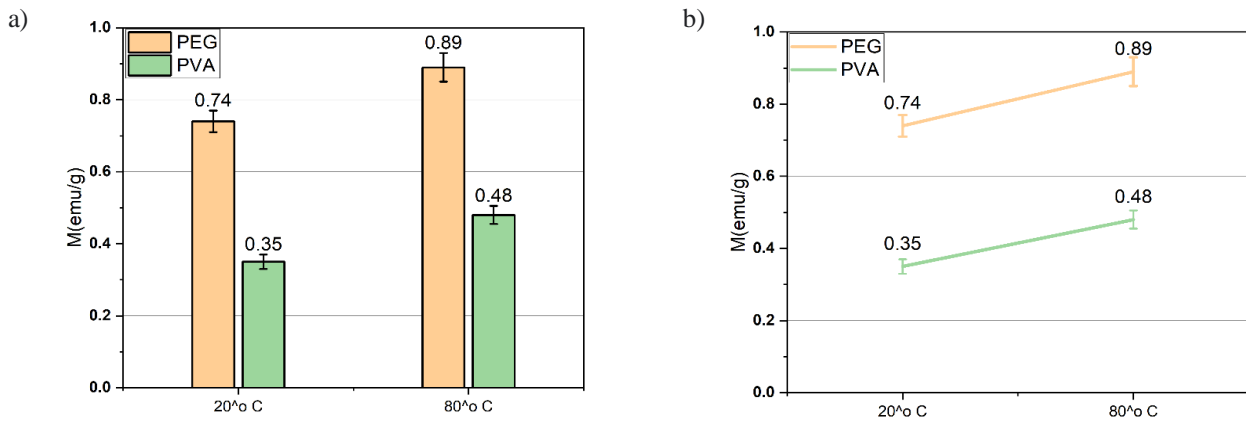| Code of experiment	a	b	c	ab	ac	bc	abc	Response		
								M_s	M_r	H_c
Y_1	-1	-1	-1	+1	+1	+1	-1	32/39	0/41	6/95
Y_a	+1	-1	-1	-1	-1	+1	+1	49/36	0/72	0/72
Y_b	-1	+1	-1	-1	+1	-1	+1	9/59	0/41	5/95
Y_c	-1	-1	+1	+1	-1	-1	+1	49/39	1/80	37/90
Y_{ab}	+1	+1	-1	+1	-1	-1	-1	15/00	0/29	7/83
Y_{ac}	+1	-1	+1	-1	+1	-1	-1	60/94	1/63	16/6
Y_{bc}	-1	+1	+1	-1	-1	+1	-1	10/46	0/64	29/6
Y_{abc}	+1	+1	+1	+1	+1	+1	+1	20/45	0/04	16/30
Average of central point	0	0	0	0	0	0	0	28/86	1/68	28/80

Fig. 8: Investigation of the effect of coating agent and temperature on magnetic remanent.

STATISTICAL CHARACTERIZATION OF THE M_s AND M_r

The magnetic behavior of the coated MNPs was investigated by VSM instrument, and saturation magnetization (M_s), remnant magnetism (M_r) and magnetic coercivity (H_c) were determined. The results of the set of experiments carried out within the frame of two-level factorial design are recorded in Table 2.

Hysteresis diagrams (Fig. 9 and 10) show the effect of three factors of alkali solution strength, polymer agent and temperature on the magnetic behavior of coated magnetic nanoparticles (based on the experiment's code of Table 2).

Comparison of the hysteresis diagram of the samples shows the effect of high temperature (80 °C), the strength of the strong alkaline solution (ammonia) and the polymeric agent PEG on the magnetic properties of the magnetic nanoparticles.

The average effects of the factors and the interaction effects computed Eq. (5), and they recorded in Table 3.

$$\text{Effect} = \frac{\sum \text{posetive level} - \sum \text{negative level}}{4} \quad (5)$$

For example, the M_s increases, on the average, by 6.225 emu/g by changing temperatures from 20° to 80°. Also, as the strength of the alkaline solution increases (using ammonium solution instead of sodium hydroxide), the M_s increases to an average of 13.48 emu/g. Each of the calculated values, should be compared with the variance to evaluates their coefficients. The standard deviation of each effect is determined by comparing

Table 3: Calculated effects for selected factors and interaction between them.

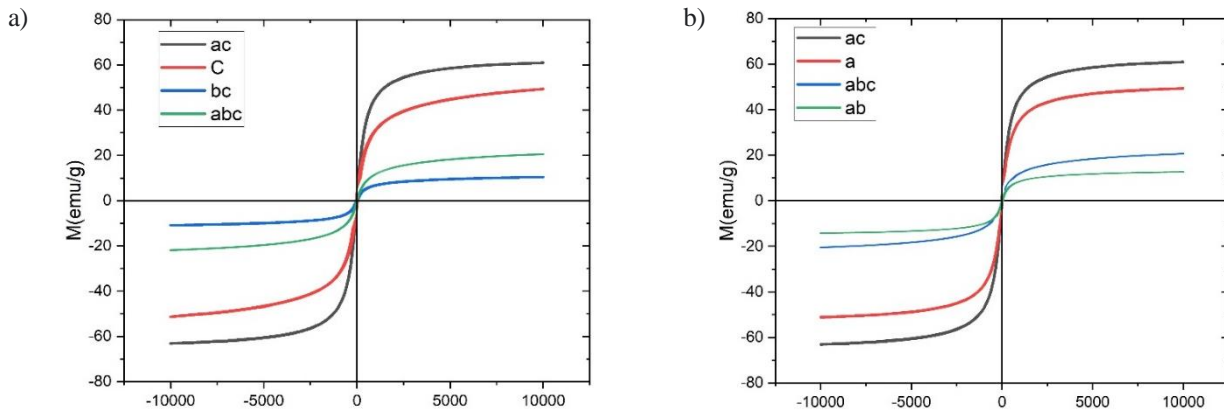| Factors	A	B	C	AB	AC	BC	ABC
Effect M_s(emu/g)	13.48	-31.645	6.225	-0.78	-2.71	-8.065	-7.1×10^{-15}
Effect M_r(emu/g)	-0.145	-0.795	0.57	-0.215	-o.24	-0.58	1.1×10^{-15}
Effect H_r(G)	-9.74	-0.61	19.79	4.055	-7.56	-3.66	-1.2×10^{-15}

a)

b)

Fig. 9: (a) The effect of alkali solution strength and coating agent on the magnetic behavior of nanoparticles at 80 °,
(b) the effect of temperature and coating factor on magnetic behavior of nanoparticles in alkaline ammonia environment.
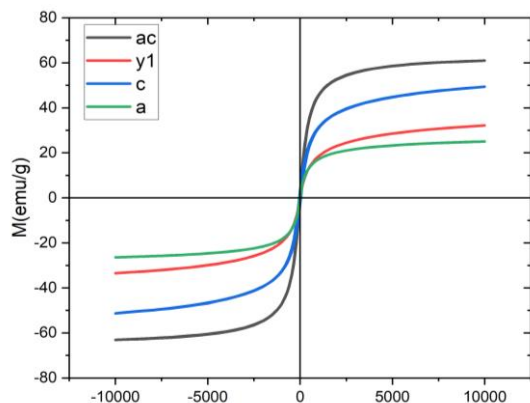

Fig. 10: The effect of temperature and strength of alkaline solution on the magnetic behavior of nanoparticles with PEG coating.

the standard deviation of the experimental calculations [40,50,51]. By comparing the results of two repetitions of the central point measurement with other measurements, can be calculated the standard deviation of each effect. The value of this quantity for saturation magnetization is equal to $0.37 (S^2 =0.37)$. This quantity depends on the variance of each effect according to the following equation:

$$S^2_{effect} = \frac{4S^2}{N} \quad \text{(N is number replicate measurements)}$$

Confidence interval = effect $\mp t_{\alpha\,2n}\,S_{effect}$. If N=8, $\alpha = 0.05$, for df=8, the tabulated value is $t_{0.05/2}$ =2.3. therefore effect $\mp\,2.3 \times 0.534 =$ effect ∓ 1.23. The confidence intervals of A, B, C and BC effects will not include zero, because the absolute value of the saturation magnetization(M_s) of each is greater than 1.23. These should be considered as significant effects on the amount of saturation magnetization of the coated MNPs.

According to calculations, If the process of synthesis of modified MNPs is performed in ammonium solution (instead of sodium hydroxide solution), the amount of saturation magnetization of the nanoparticles will increase significantly (13.48emu/g). By using PVA polymer agent instead of PEG, the amount of saturation magnetization is significantly reduced (-31.645). The synthesis of coated MNPs at high temperatures (80°) causes a noticeable increase in saturation magnetization (6.22emu/g).

Fig. 11, shows the normal probability diagram for the data. As it clear, the factors A, B and C and interaction BC, affect the results of the saturation magnetization of the modified MNPs and the other interactions can be ignored.
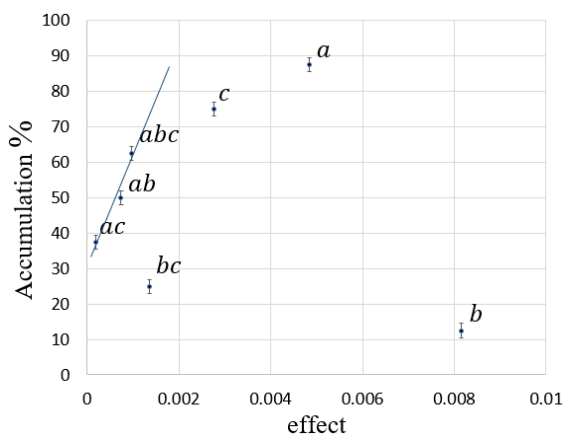
Fig. 11: Normal probability (%) of the effects.

In this study, there is no correlation between the variables in this two-level design. In the two-level factorial design, there is no correlation between these variables. They are orthogonal and form a diagonal matrix.

One of the main applications of magnetic nanoparticles in metal adsorption industry, which saves money and time. Each nanoparticle; It absorbs the desired cations from the solution and then the nanoparticles are collected by the magnetic field. Residual water is directed outwards, in the next step it is added to the nanoparticles of the spiriting agent solution, by removing the field and disperse, the nanoparticles disperse (in which case the stripping agent works better). Then, by reactivating the magnetic field, the nanoparticles collected and the remaining solution containing the desired metal ions are obtained in a purer form. So, the softer the magnetic nanoparticles and the higher the saturation magnetization, the absorption process can be performed with less energy consumption in a shorter time and at a higher speed.

CONCLUSIONS

The results indicate that this new design (two-level factorial design) used in the modification and optimization of magnetic nanoparticles has been significantly effective. Polymeric agents used to stabilize magnetic nanoparticles have a significant effect in hard conditions and reduce their size. Existence of electrostatic attraction and stronger hydrogen bonds between the PEG and the surface of the MNPs cause the polymeric agent to stick to the surface of the nanoparticles and not easily separate from the surface, thus this agent shows better performance than PVA. Chemical reactions were performed more completely at high temperatures (80 ºC) and the process of aligning the magnetic moments was caried out better. Ammonia alkaline solution had a significant effect on modifying and optimizing the magnetic properties of magnetic nanoparticles.

REFERENCES

[1] Arosio p., Applications and Properties of Magnetic Nanoparticles, *Nanomaterials*, **11**: 1297 (2020). Doi: 10.3390/nano11051297

[2] Khan P.L., Saeed K., Khan I., Nanoparticles: Properties, Applications and Toxicities, *Arabian Journal of Chemistry.*,**12(7)**: 908-931 (2019) doi: 10.1016/j.arabjc.2017.05.011

[3] Monsalve A., Vicente J., Grippin A., Dobson J., Poly (Lactic Acid) Magnetic Microparticle Synthesis and Surface Functionalization IEEE, *Magnetics Letters*, **8** (2017). doi: 10.1109/LMAG.2017.2726505.

[4] Bansal R., Gronkiewicz B., Storm G., Prakash J., Relaxin-Coated Superparamagnetic Iron-Oxide Nanoparticles as a Novel Theranostic Approach for the Diagnosis and Treatment of Liver Fibrosis, *J. Hepatol.*, **66(1)** (2017). DOI: 10.1016/S0168-8278(17)30348-3

[5] Ali A., Zafar H., Zia M., Ul Haq I., Phull A.R., Sarfraz Ali J., Hussain A., Synthesis, Characterization, Applications, and Challenges of Iron Oxide Nanoparticles, *Nanotechnol Sci Appl.*, **2016(9):** 49-61 (2016) doi: 10.2147/NSA.S99986

[6] Mohammed L., Gomaa H.G., Ragab D., Zhu J., Magnetic Nanoparticles for Environmental and Biomedical Applications: A Review, *Particuology,* **30** (2017) DOI: 10.1016/j.partic.2016.06.001

[7] Farahmandjou M., Khodadadi A., Yaghoubi M., Synthesis and Characterization of Fe-Al2O3 Nanoparticles Prepared by Coprecipitation Method, *Iranian Journal of Chemistry and Chemical Engineering (IJCCE),* **40(3)**: 725-730 (2021).
DOI: 10.30492/ijcce.2020.38036

[8] T. Poursaberi, V. Akbar, S.M.R. Shoja, Application of Rh(III)-Metalloporphyrin Grafted Fe3O4 Nanoparticles for the Extraction of Thiocyanate Ions from Aqueous Solutions, *Iranian Journal of Chemistry and Chemical Engineering (IJCCE)*, **34(2)**: 41-49 (2015).
DOI: 10.30492/ijcce.2015.14095

[9] Karimzadeh I., Aghazadeh M., Dalvand A., Doroudi T., Kolivand P. H., Ganjali M. R., Norouzi P., Effective Electrosynthesis and in Situ Surface Coating of Fe_3O_4 Nanoparticles with Polyvinyl Alcohol for Biomedical Applications, *Materials Research Innovations,* **23(1)***: 1-8(2019)

[10] S.H. Ahmadi, P. Davar, A. Manbohi, Adsorptive Removal of Reactive Orange 122 from Aqueous Solutions by Ionic Liquid Coated Fe_3O_4 Magnetic Nanoparticles as an Efficient Adsorbent, *Iranian Journal of Chemistry and Chemical Engineering (IJCCE),* **35(1)**: 63-73 (2016).
DOI: 10.30492/ijcce.2016.18809

[11] Aghazadeh M., Karimzadeh I., Ganjali M. R., Preparation and Characterization of Amine- and Carboxylic Acid-functionalized Superparamagnetic Iron Oxide Nanoparticles Through a One-step Facile Electrosynthesis Method, *Bentham Science Publishers*, **15(2)**: 169-177 (2019)
doi:10.2174/1573413714666180622150216

[12] Suzdalev I. P., Maksimov Yu. V., Imshennik V. K., Novichikhin S.V., Matveev V.V., Tret'yakov Yu. D., Lukashin A.V., Eliseev A.A., Avramenko N.V., Malygin A.A., Sosnov E.A., Formation and Properties of the Nanocluster Structure of Iron Oxides, *Russian Chemical Bulletin* **55**: 1755–1767 *(2006).*

[13] Khodadadi A., Talebtash M.R, Investigation and Synthesis of Fe Doped Al_2O_3 Nanoparticles by Co-Precipitation and Sol Gel Methods, *Asian Journal of Nanosciences and Materials,* **6(2)**: (2022).

[14] Trukhanov A.V., Kostishyn V.G., Panina L.V., Korovushkin V.V., Turchenko V.A., Thakur P., Thakur A., Yang Y., Vinnik D.A., Yakovenko E.S., Matzui L.Y., Trukhanova E.L., Trukhanov S.V., Control of Electromagnetic Properties in Substituted M-Type Hexagonal Ferrites, *Journal of Alloys and Compounds,* **754**: 247-256 (2018)
doi: 10.1016/j.jallcom.2018.04.150.

[15] Dukenbayev K., Korolkov I.V., Tishkevich D.I., Kozlovskiy A.L., Trukhanov S.V., Gorin Y.G., Shumskaya E.E., Kaniukov E.Y., Vinnik D.A., Zdorovets M.V., Anisovich M., Trukhanov A.V., Tosi D., Molardi C., Fe_3O_4 Nanoparticles for Complex Targeted Delivery and Boron Neutron Capture Therapy, *Nanomaterials*, **9**:494 (2019)
https://doi.org/10.3390/nano9040494

[16] Farahmandjou M., Soflaee F., Synthesis and Characterization of α-Fe_2O_3 Nanoparticles by Simple Co-Precipitation Method, *Phys. Chem. Res.* **3**: 193 (2015)
doi: 10.22036/PCR.2015.9193.

[17] Effenberger F. *et al*, Effenberger F B, Couto R A, Kiyohara P K., Economically Attractive Route for the Preparation of High-Quality Magnetic Nanoparticles by the Thermal Decomposition of Iron (III) Acetylacetonate, *Nanotechnology,* **28**: 115603 (2017)
Doi: 10.1088/1361-6528/aa5ab0

[18] Patselas V., Kosinová L., Lovri M., Ferhatovic L., Rabyk M., Konefal R., Paruzel A., Šlouf M., Heryenk V., Gajović S., Horák D., Superparamagnetic Fe_3O4 Nanoparticles: Synthesis by Thermal Decomposition of Iron (III) Glucuronate and Application in Magnetic Resonance Imaging, *ACS Appl. Mater. Interfaces,* **8**: 7238-7247 (2016)
doi: 10.1021/acsami.5b12720.

[19] M. Farahmandjou, S.A. Salehizadeh, The Optical Band Gap and the Tailing States Determination in Glasses of TeO_2-V_2O_5-K_2O System, *Glass Phys. Chem.,* **39**:473 (2013)
doi: 10.1134/S1087659613050052.

[20] Albert E.L., Che Abdullah C.A., Shirataki Y., Synthesis and Characterization of Graphene Oxide Functionalized with Magnetic Nanoparticle *via* Simple Emulsion Method, *Results Phys.,* **11**: 944-950 (2018)
doi: 10.1016/j.rinp.2018.10.054.

[21] Farahmandjou M., Honarbakhsh S., Behrouzinia S., PVP-Assisted Synthesis of Cobalt Ferrite (CoFe$_2$O$_4$) Nanorods, *Phys. Chem. Res.,* **4**: 655 (2016) doi: 10.22036/pcr.2016.16702.

[22] Ali A., Rehmat S., Zhou P., Guo K., Ovais M., Rehmat, Review on Recent Progress in Magnetic Nanoparticles: Synthesis, Characterization, and Diverse Applications, *Front Chem.*, **9** :629054 (2021). doi: 10.3389/fchem.2021.629054

[23] Khodadadi A., Talebtash M.R., Farahmandjou M., Effect of PVA/PEG-coated Fe$_3$O$_4$ Nanoparticles on the Structure, Morphology and Magnetic Properties, *Physical Chemistry Research*, **10**: 537 (2022). doi: 10.22036/pcr.2022.326878.2023

[24] Bajaj N.S., Joshi R.A., The Coprecipitation is the Simplest Way to Prepare Iron Oxide Nanoparticles of Magnetite (Fe$_3$O$_4$). In "Handbook of Nanotechnology Application" (2021).

[25] Chu X., Hou Y.L., Magnetic Nanomaterials: Fundamentals, Synthesis and Applications. In Y. L. Hou, D. J. Selmer (Eds.), "Overview of Synthesis of Magnetic Nanomaterials", John Wiley & Sons, Inc., 83-120 (2017).

[26] Koo K., Ismail A.E., Othman M.D., Bidin N., Rahman M., Preparation and Characterization of Superparamagnetic Magnetite (Fe$_3$O$_4$) Nanoparticles: A Short Review, *Malaysian J. Fund. Appl. Sci.,* **15**: 23-31 (2019). doi: 10.11113/mjfas.v15n2019.1224.

[27] Yeap S.P., Lim L.K., Ooi B.S., Ahmad A.A*., Agglomeration, Colloidal Stability, and Magnetic Separation of Magnetic Nanoparticles: Collective Influences on Environmental Engineering Applications, *J. Nanoparticle. Res.*, **19**: 368 (2017) doi: 10.1007/s11051-017-4065-6.

[28] Yu S.M., Romaine A.LA., Roig A., Enhanced Stability of Superparamagnetic Iron Oxide Nanoparticles in Biological Media Using a pH Adjusted-BSA Adsorption Protocol, *J. Nanoart. Res.*, **16**: 2484 (2014) doi: 10.1007/s11051-014-2484-1

[29] Tishkevich D.I., Korolkov I.V., et al., Immobilization of Boron-Rich Compound on Fe$_3$O$_4$ Nanoparticles: Stability and Cytotoxicity, *Journal of Alloys and Compounds*, **797**: 573-581 (2019).

[30] Trukhanov S.V., Trukhanov A.V., et al, Polarization Origin and Iron Positions in Indium Doped Barium Hexaferrites, *Ceramics International*, **44**: 290-300 (2018).

[31] Ahrberg C.D, Choi J.W., Chung B.G., Automated Droplet Reactor for the Synthesis of Iron Oxide/Gold Core-Shell Nanoparticles, *Sci. Rep.*, **10**: 1737 (2020). doi: 10.1038/s41598-020-58580-9.

[32] Salehipour M., Rezaei S., safer J., Pakdin-Parizi Z., Recent Advances in Polymer-Coated Iron Oxide Nanoparticles as Magnetic Resonance Imaging Contrast Agents, *J. Nanoparticle Res.*, **23** (2021). Doi: 10.1007/s11051-021-05156-x.

[33] Ganesha A., Edi S., A Synthesis of Polyethylene Glycol (PEG)-Coated Magnetite Fe$_3$O$_4$ Nanoparticles and Their Characteristics for Enhancement of Biosensor, *Mater. Res. Express,* **7(5)**: (2020).

[34] Maleki A., Niksefat M., Rahimi J., Hajizadeh Z., Design and Preparation of Fe$_3$O$_4$@PVA Polymeric Magnetic Nanocomposite Film and Surface Coating By Sulfonic Acid via in Situ Methods and Evaluation of its Catalytic Performance in the Synthesis of Dihydropyrimidines, *BMC Chemistry,* 13 (2019)

[35] Grize Y.L., A Review of Robust Process Design Approaches, *J. Chemom.*, **9**: 239 (1995). Doi: 10.1002/cem.1180090402

[36] Kalil S.J., Maugeri F., Rodrigues M.I., Response Surface Analysis and Simulation as a Tool for Bioprocess Design and Optimization, *Process Biochem.*, **35(6)**: (2000). Doi: 10.1016/S0032-9592(99)00101-6

[37] Gheshlagi R., Scharer J.M., Moo-young M., Douglas P.L., Application of Statistical Design for the Optimization of Amino Acid Separation by Reverse-Phase HPLC, *Biochem.*, 383 (2008). DOI: 10.1016/j.ab.2008.07.032

[38] Sadeghi S., Azhdari H., Arabi H., Moghaddam A.S., Surface Modified Magnetic Fe$_3$O$_4$ Nanoparticles as a Selective Sorbent for Solid Phase Extraction of Uranyl Ions from Water Samples, *Journal of Hazardous Materials*, 215 (2012). Doi: 10.1016/j.jhazmat.2012.02.054

[39] Behnam-Saba A.R., Saberyan K., Nezhadali A., Adelkhani H., A Chemometric Study of the Adsorption of Zr(IV) Ions from Aqueous Solutions onto TBP-Surface-Modified Magnetic Fe$_3$O$_4$ Nanoparticles as a New Adsorbent, *Radiochemistry*, **62**: 62-72 (2020). Doi: 10.1134/s1066362220010087

[40] Massart D. L., Vandeginste B.G.M., Buydens L.M.C., De Jong S., Lewi P. J., Smeyers-Verbeke J., Handbook of Chemometrics and Qualimetrics: *Part A, J. Chem. Inf. Comput. Sci.*, **38(6)**: 1254 (1998).
doi: 10.1021/ci980427d

[41] Scherrer p., Bestimmung Der inneren Struktur und der Größe von Kolloidteilchen Mittels Röntgenstrahlen, Mathematisch- Physikalische Klasse, 2 (1918)

[42] Karimzadeh I., Aghazadeh M., Davoudi T., Ganjali M.R., Koliva P.H., Superparamagnetic Iron Oxide (Fe3O4) Nanoparticles Coated with PEG/PEI for Biomedical Applications: A Facile and Scalable Preparation Route Based on the Cathodic Electrochemical Deposition Method, *Adv. Phys. Chem.*, 2017 (2017).
doi: 10.1155/2017/9437487.

[43] Farahmandjou M., Jurablu S., Co-precipitation Synthesis of Zinc Oxide (ZnO) Nanoparticles by Zinc Nitrate Precursor, *Int. J. Bio-Inorg. Hybr. Nanomater.,* 3 (2014)

[44] Shokrollahi H., A Review of the Magnetic Properties, Synthesis Methods and Applications of Maghemite, *J. Magnet. Mater*., 426 (2017).
doi: 10.1016/j.jmmm.2016.11.033.

[45] Khodadadi A., Farahmandjou M., Yaghoubi M., Investigation on Synthesis and Characterization of Fe-doped Al2O3 Nanocrystals by New Sol–Gel Precursors, *Mater. Res. Express*., **6(2)** (2018).
doi: 10.1088/2053-1591/aaef70.

[46] Assay F., Jafarizadeh Malmiri H., Ajamein H., Anarjan N., Vaghari H., Sayyar Z., Berenjian A., A biotechnological Perspective on the Application of Iron Oxide Nanoparticles, *Nano Res.,* **9**: 2203-2225 (2016).
doi: 10.1007/s12274-016-1131-9

[47] Liu B., Wang D., Huang W., Yao A., Kamitakahara M., Ioku K., Preparation of Magnetite Nanoparticles Coated with Silica via a Sol-Gel Approach, *Journal of the Ceramic Society of Japan,* 115 (2007)

[48] Businova P. Chomoucka J., Prasek J., Hrdy R., Drbohlavova J., Sedlacek P., Hubalek J., Polymer Coated Iron Oxide Magnetic Nanoparticles: Preparation and Characterization, *Nanocon*, 9 (2011)

[49] Anil A.C., Govindan K., Rangarajan M., Synthesis of Poly (Ethylene Glycol) (PEG)-Capped Fe$_3$O$_4$ Nanoclusters by Hydrothermal Method, *Materials Science and Engineering*, 577 (2019).
doi:10.1088/1757-899X/577/1/012153

[50] Schoenmakers P.J., Bartha A., Billiet H., Gradien Elution Methods for Predicting Isocratic Conditions, *J. Chromatogr.,* 550 (1991).
doi: 10.1016/s0021-9673(01)88554-X

[51] Mahadevan S., Gnanaprakash G., Philip J., Rao B.P.C., Jayakumar T., X-Ray Diffraction-Based Characterization of Magnetite Nanoparticles in Presence of Goethite and Correlation with Magnetic Properties, *Physica E: Low-Dimensional Systems and Nanostructures*, 39 (2007).
doi: 10.1016/J.Physe.2006.12.041